Study of Plasmachemical Synthesis of Fuel Compositions for Dispersion Nuclear Fuel

Alexander Karengin
School of Nuclear Science and Engineering
Tomsk Polytechnic University
Tomsk, Russia
karengin@tpu.ru

Ivan Novoselov
School of Nuclear Science and Engineering
Tomsk Polytechnic University
Tomsk, Russia
inovoselov@tpu.ru

Igor Shamanin
School of Nuclear Science and Engineering
Tomsk Polytechnic University
Tomsk, Russia
shiva@tpu.ru

Alexey Tikhonov
School of Nuclear Science and Engineering
Tomsk Polytechnic University
Tomsk, Russia
aet13@tpu.ru

Nikita Golovkov
School of Nuclear Science and Engineering
Tomsk Polytechnic University
Tomsk, Russia
golniigo@gmail.com

***Abstract*—The paper presents the results of studies of the plasmachemical synthesis of fissile material (uranium dioxide) and the matrix (yttria) for dispersion nuclear fuel. For this purpose, simulated water-organic solutions of zirconyl nitrate, yttrium nitrate and organic component (acetone) have been used. For the first time, the compositions of such solutions and the modes of their processing, which ensure the synthesis of nanosized oxide powders in air plasma, were determined.**

***Keywords*—plasma, plasmachemical synthesis, fuel composition, fissile material, matrix, dispersive nuclear fuel, water-organic nitrate solution**

I. INTRODUCTION

For nuclear power engineering, the use of dispersive nuclear fuel (NF), in which there are no direct contacts between particles of fissile material (uranium dioxide enriched in the uranium-235 isotope), is promising due to their uniform distribution in the matrix with high thermal conductivity and low neutron absorption [1-5].

The advantages of plasmachemical synthesis of zirconia and yttria from water nitrate solutions (WNS) are [6-8]: single-stage and high-speed process, homogeneous phase distribution with a required stoichiometric composition, the ability to influence particle size and morphology, the compactness of process equipment, and low cost. However, WNS plasma processing requires a significant amount of electrical energy (up to 4.0 kWh/kg). A significant reduction in energy consumption (from 4.0 to 0.1 kW·h/kg) can be achieved by plasma processing of WNS solutions along with any organic component (alcohols, ketones, etc.) in the form of water-organic nitrate solution of optimal composition (WONS) [9].

The purpose of this work is to determine the possibility of plasmachemical synthesis of zirconia (an simulator of fissile material - uranium dioxide) and yttria (matrix) in air plasma from WONS.

To achieve the goal, the following tasks were defined: determination of the composition of WONS and their plasma processing modes, which ensure plasmachemical synthesis of zirconia and yttria in air plasma; research of their physical and chemical properties; confirmation of nanoscale class of obtained powders.

II. CALCULATION OF BURNING PARAMETERS OF WONS

Lower heat value of WONS is determined from equation [10].

$$Q_l = \frac{(100 - W - A)\cdot Q_{lc}}{100} - \frac{2.5\cdot W}{100}, \quad (1)$$

where Q_{lc} is lower heat value of combustible component of WONS, MJ/kg; W and A are content of water and noncombustible components, wt.%; 2,5 is the value of latent heat of vaporization for water at 0 °C, MJ/kg.

Energy-efficient processing of solutions containing any organic component is achieved with a lower heat value of minimum 8.4 MJ/kg [10].

Tables 1 and 2 show the effect of the content of the organic component (acetone) on the lower heat value of WONS "water-acetone-yttrium nitrate" and "water-acetone-zirconyl nitrate".

TABLE I. THE EFFECT OF THE CONTENT OF THE ACETONE ON THE LOWER HEAT VALUE OF WONS "WATER-ACETONE-YTTRIUM NITRATE"

C_3H_6O, %	H_2O, %	$Y(NO_3)_3{\cdot}6H_2O$, %	Q_{lc}, MJ/kg
10	45.8	44.2	1.5
30	35.6	34.4	7.1
35	**33.0**	**32.0**	**8.4**
50	25.4	24.6	12.7
70	15.2	14.8	18.4
90	5.1	4.9	24.0

TABLE II. THE EFFECT OF THE CONTENT OF THE ACETONE ON THE LOWER HEAT VALUE OF WONS "WATER-ACETONE-ZIRCONYL NITRATE"

C_3H_6O, %	H_2O, %	$ZrO(NO_3)_2{\cdot}2H_2O$, %	Q_{lc}, MJ/kg
10	57.4	32.6	1.2
30	44.7	25.3	6.9
36	**40.8**	**23.2**	**8.4**
50	31.9	18.1	12.6
70	19.1	10.9	18.3
90	6.4	3.6	24.0

Taking into account the obtained results, the following WONS compositions having a $Q_{lc} \approx 8.4$ MJ/kg were determined:

- composition of WONS-1: 33.0 % H_2O : 35.0 % C_3H_6O : 32.0 % $Y(NO_3)_3{\cdot}6H_2O$;
- composition of WONS-2: 40.8 % H_2O : 36.0 % C_3H_6O : 32.0 % $ZrO(NO_3)_2{\cdot}2H_2O$.

978-1-7281-2896-2/19/$31.00 ©2019 IEEE

III. THERMODYNAMIC MODELING OF PLASMACHEMICAL SYNTHESIS OF YTTRIA AND ZIRCONIA

To determine the optimal modes of the process under study, equilibrium compositions of gaseous and condensed products of plasma processing of WONS-1 and WONS-2 were calculated. For the calculations, a licensed program "TERRA" for the thermodynamic calculation of the phase composition of heterogeneous systems was used. The calculations were carried out at atmospheric pressure (0.1 MPa), for a wide range of temperatures (300–4000 K) and mass fractions of the air plasma coolant (0.1–0.95).

To choose the optimal process mode, there are several factors to be considered. The first one is that the adiabatic temperature of WONS plasma processing should be minimum 1200 °C in order to ensure complete combustion of the organic component to CO_2 and H_2O. The second one is the minimum fraction of the air coolant, which ensures the maximum yield of the product without the formation of carbon (soot) in plasma treatment products.

Calculation of adiabatic temperature of WONS plasma processing was carried out with the following formula [9]:

$$T_{ad} = \frac{Q_l + C_{mix} \cdot t_{mix} + \alpha \cdot \upsilon_{ox} \cdot C_{ox} \cdot t_{ox}}{V \cdot C}, \qquad (2)$$

where Q_l is Lower heat value of WONS, kJ/kg; C_{mix} is average mass heat capacity of WONS, kJ/(kg·grad); t_{mix} is temperature of WONS, °C; α is oxidant flow coefficient; υ_{ox} is theoretical flow of oxidant, m^3/m^3; C_{ox} is average heat capacity of oxidizer, $(kJ/m^3 \cdot grad)$; t_{ox} is temperature of oxidizer, °C; V is specific volume of gaseous and condensed products, m^3/kg; C is specific equilibrium heat capacity of gaseous and condensed products, $(kJ/m^3 \cdot grad)$.

Table 3 shows the effect of the air mass fraction on the adiabatic temperature of the WONS-1 plasma processing.

TABLE III. EFFECT OF THE AIR MASS FRACTION ON THE ADIABATIC TEMPERATURE OF THE WONS-1 "WATER-ACETONE-YTTRIUM NITRATE"

Air, %	H_2O, %	$Y(NO_3)_3 \cdot 6H_2O$, %	C_3H_6O, %	T_{ad}, MJ/kg
50	16.5	16.0	17.5	892
60	13.3	12.7	14.0	1029
68	10.6	10.2	11.2	1181
69	**10.2**	**9.9**	**10.9**	**1212**
70	9.9	9.6	10.5	1222
50	16.5	16.0	17.5	892

Fig. 1 shows the effect of temperature on the equilibrium compositions of the main gaseous (a) and condensed (b) products of WONS-1 plasma processing at air mass fraction of 69 %.

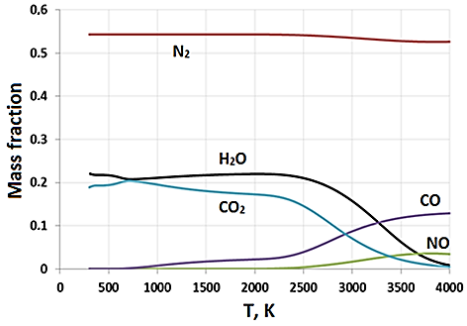

a)

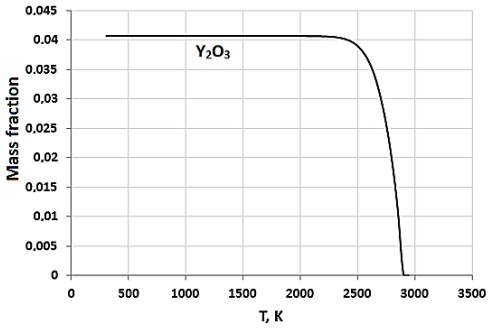

b)

Fig. 1. Effect of temperature on the equilibrium compositions of the main gaseous (a) and condensed (b) products of WONS-1 plasma processing at air mass fraction of 69 %

From the analysis of Table 3 and in Fig. 1, it follows that the air mass fraction of 69 % ensures the production of the product in the condensed phase (marked "c") as Y_2O_3(c) in a wide temperature range without the formation of carbon C(c). The decrease in the mass fraction of air below 69 % leads to the formation and a sharp increase of the carbon content C(c) in the composition of the products. The increase in the proportion of air above 69 % does not change the composition of the products in the condensed phase, but leads to a decrease of the mass fraction of the yttria product.

Table 4 shows the effect of the air mass fraction on the adiabatic temperature of the WONS-2 plasma processing.

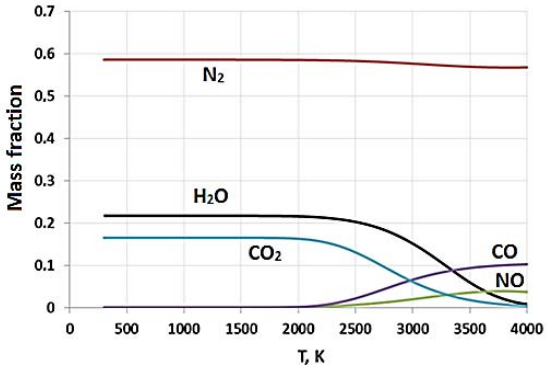

a)

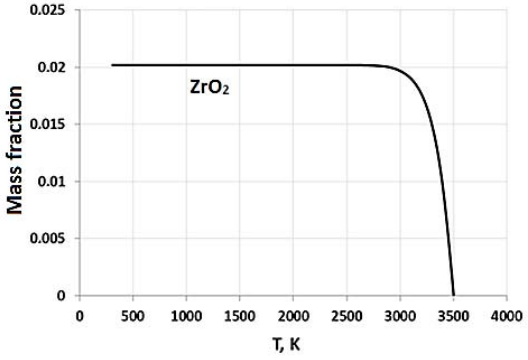

b)

Fig. 2. Effect of temperature on the equilibrium compositions of the main gaseous (a) and condensed (b) products of WONS-2 plasma processing at air mass fraction of 76 %

From the analysis of Table 4 and in Fig. 2, it follows that the air mass fraction of 76 % ensures the production of the product in the condensed phase as ZrO_2(c) in a wide

temperature range without the formation of carbon C(c). The decrease in the mass fraction of air below 76 % leads to the formation and a sharp increase of the carbon content C(c) in the composition of the products. The increase in the proportion of air above 76 % does not change the composition of the products in the condensed phase, but leads to a decrease of the mass fraction of the zirconia product.

IV. Routine of Experiment

Experimental studies of the process of plasmachemical synthesis of yttria and zirconia from dispersed WONS were carried out with the help of a laboratory plasma stand "Plasma Module Based on a High-Frequency Generator HFG8-60/13-01", which is shown in Fig. 3 [11,12].

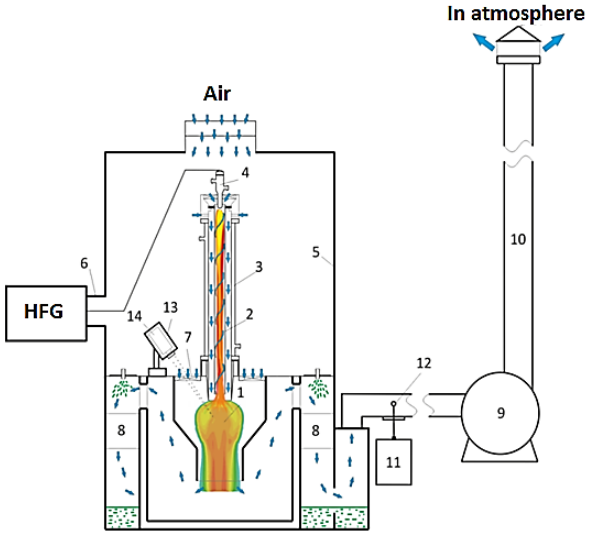

Fig. 3. Scheme of laboratory plasma stand "Plasma module based on high frequency generator HFG8-60/13-01": 1 – disperser; 2 – HF torch discharge; 3 – high-frequency torch plasmatron; 4 – copper electrode; 5 – case; 6 – coaxial output; 7 – reactor; 8 – assembly for gas scrubbing; 9 – air exhauster; 10 – gas duct; 11 – gas analyzer; 12 – air sampling; 13 – pyrometer protection cover; 14 – pyrometer; HFG – high frequency generator

To prepare WNS yttrium nitrate ($Y(NO_3)_3 \cdot 6H_2O$) and zirconyl nitrate ($ZrO(NO_3)_2 \cdot 2H_2O$) were used. These salts were dissolved in water according to their solubility values (96.7 g/100 ml of water and 56.67 g/100 ml of water respectively). Further, these solutions were mixed with acetone in the required proportion (Tables 3,4) to form WONS-1 and WONS-2.

Prepared solutions (WONS-1 and WONS-2) were fed separately with a constant flow rate of 0.55 kg/s (WONS-1) and 0.40 kg/s (WONS-2) to the disperser 1 and then dispersed into the reactor, where plasmachemical synthesis of yttria and zirconia was carried out at a temperature of about 1200 °C. Temperature in the reactor was controlled using a high-precision digital pyrometer (IPE 140/45) 14. After plasma treatment of solution in the reactor, the dust-vapor gas mixture entered the wet cleaning unit 8, where its rapid cooling (hardening) and separation of obtained powders occurred. The following analyses of these powders were conducted: scanning electron microscopy (SEM) and transmission electron microscopy (TEM) to study the morphology and particle size, BET analysis to determine the specific surface of the powder and X-ray phase analysis to study the phase composition of the obtained powders.

V. Analysis of Yttria and Zirconia Powders

Phase composition of obtained powders was measured using X-ray diffractometer Shimadzu XRD-7000. Fig. 4 shows the phase composition of samples of powders obtained from WONS-1 (a) and WONS-2 (b).

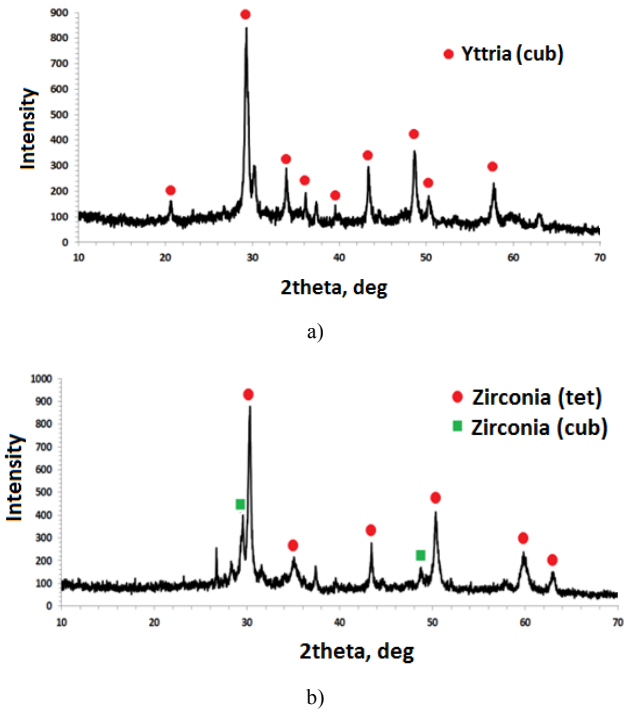

Fig. 4. X-ray diffraction patterns of powder samples obtained from WONS-1 (a) and WONS-2 (b)

X-ray analysis of the sample of powder obtained from WONS-1 (Fig. 4a) shows that yttria is in the cubic phase. X-ray analysis of the sample of powder obtained from WONS-2 (Fig. 4b) shows that zirconia is in the tetragonal and cubic phase.

JEOL JSM-7500FA scanning electron microscope was used to study the particle size and morphology in obtained powders.

Fig. 5 shows SEM micrographs of particles of yttria (a) and zirconia (b) powders.

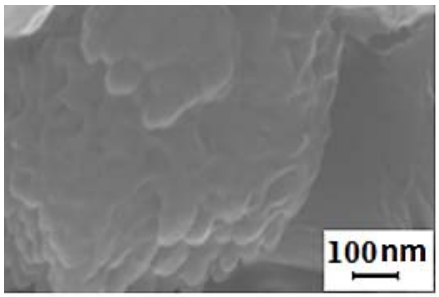

a)

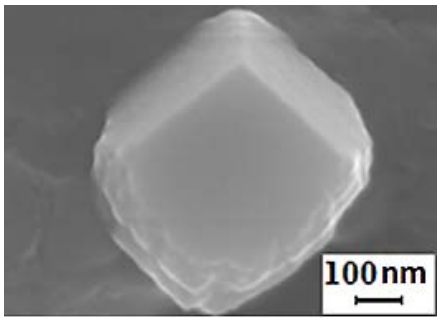

b)

Fig. 5. SEM micrographs of particles of yttria (a) and zirconia (b) powders

Analysis of the morphology of the yttria particles from (Fig. 5a) shows that the powder consists of agglomerates, including grains 40-60 nm in size. Analysis of the morphology of the zirconia particles from (Fig. 5b) shows that the powder consists of agglomerates, including grains 60-110 nm in size. Therefore both powders can be classified as nanosized.

To construct histograms of particle size distribution, transmission electron microscopy was performed using a Philips CM-12 TWIN electron microscope. Fig. 6 shows TEM micrographs of particles of yttria (a) and zirconia (b) powders.

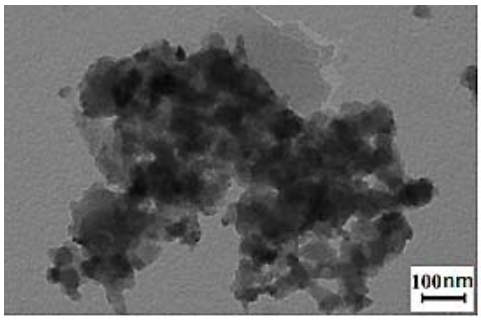

a)

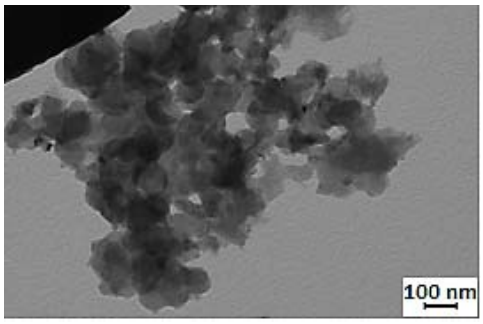

b)

Fig. 6. TEM micrographs of particles of yttria (a) and zirconia (b) powders

A size of about a thousand particles of each powder was measured, and histograms of the particle size distribution were built on the basis of measurements (Fig. 7).

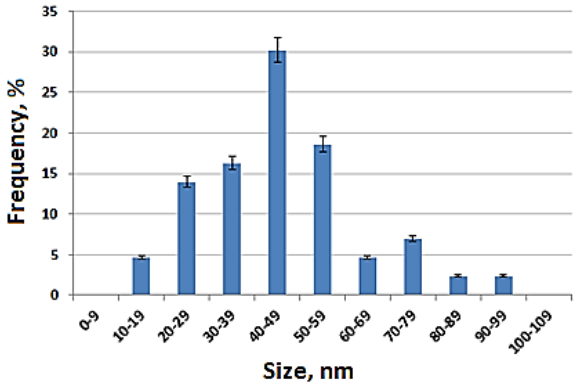

a)

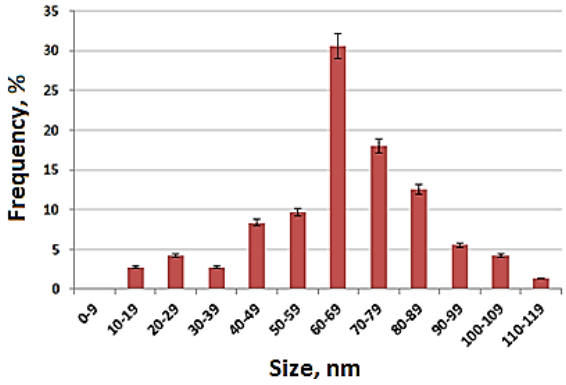

b)

Fig. 7. Particle size distribution of yttria (a) and zirconia (b) powders

The particle size distributions of the powders are close to normal. The powders contain particles with sizes of 10–100 nm (yttria), 10–120 nm (zirconia). The distribution peak (≈ 30 %) of yttria powder particles is in the range of 40–49 nm, the distribution peak (≈ 31 %) of zirconia powder particles is in the range of 60–69 nm.

Sorbi-M sorbtometer was used to analyze the specific surface area of yttria and zirconia nanopowders. The specific surface areas of yttria and zirconia are 31 and 12 m^2/g, respectively.

VI. Conclusion

As a result of the calculations of the burning parameters of the solutions “yttrium nitrate-water-acetone” and “zirconyl nitrate-water-acetone”, for the first time the optimal compositions of WONS-1 and WONS-2 having a lower heat value of about 8.4 MJ/kg and adiabatic temperature of about 1200 °C were calculated. Process conditions (mass ratio of phases, temperature) providing energy-efficient plasmachemical synthesis of yttria and zirconia were determined.

In the course of experimental studies under determined conditions, plasma processing of dispersed WONS-1 and WONS-2 and plasmachemical synthesis of yttria and zirconia were carried out for the first time.

The results of the analysis of the obtained powders confirm that the obtained powders of yttria and zirconia are nanosized.

The results of the research can be used to create technology and equipment for plasmachemical synthesis of

simple and complex nanosized oxide powders, including powders for promising types of dispersive nuclear fuel.

ACKNOWLEDGMENT

The project was supported by the Russian Science Foundation (project 18-19-00136).

REFERENCES

[1] D.M. Skorov, Yu.F. Bychkov, A.M. Dashkovskiy, Reactor material science, Atomizdat, Moscow, 1979.

[2] S.V. Alexeev, V.A. Zaytsev, S.S Tolstoukhov, Dispersive nuclear fuel, Technosphera, Moscow, 2015.

[3] C. Degueldre, J.M. Paratte. Concepts for an inert matrix fuel: An overview, Journal of Nuclear Materials, Vol. 274, 1999, pp. 1–6.

[4] Yu.N. Tuumanov, Plasma and high-frequency processes of creating and treatment of materials in nuclear fuel cycle: present and futureFizmatlit, Moscow, 2003.

[5] T. Song, Y. Wang, Z. Chang, L. Guo, In-situ fabrication of dispersion nuclear fuel pellets with a core-shell structure, Annals of Nuclear Energy, Vol. 134, 2019, pp. 258–262.

[6] A.G. Karengin, A.A. Karengin, I.Yu. Novoselov, N.V. Tundeshev, Calculation and optimization of plasma utilization process of inflammable wastes after spent nuclear fuel recycling, Advanced Materials Research, Vol. 1040, 2014, pp. 433–436.

[7] I.Yu. Novoselov, A.G. Karengin, R.G. Babaev, Simulation of uranium and plutonium oxides compounds obtained in plasma, AIP Conference Proceedings, Vol. 1938, 2018, pp. 1–5.

[8] I. Shamanin, Alexander Karengin, I. Novoselov, Alexey Karengin, E. Alyukov, A. Poberezhnikov, R. Babaev, O. Mendoza. Plasmachemical synthesis and evaluation of the thermal conductivity of metal-oxide compounds for prospective nuclear fuel, Journal of Physics: Conference Series, Vol. 1145, 2019, pp. 1–7.

[9] A.G. Karengin, A.A. Karengin, V.A. Vlasov, Kinetic model of evaporation of droplets dispersed in aqueous-organic compositions in an air-plasma flow, Russian Physics Journal, Vol. 58, 2015, pp. 730–736.

[10] M.N. Bernadiner, A.P, Shurygin, Fire processing and disposal of industrial waste, Khimiya, Moscow, 1990.

[11] A.G. Karengin, A.A. Karengin, I.Yu. Novoselov, N.I. Golovkov. Model of reactor for plasma treatment of dispersed water-organic nitrate solutions of metals, AIP Conference Proceedings, Vol. 2101, 2019, pp. 1–6.

[12] I.V. Shamanin, A.G. Karengin, A.A. Karengin, I.Yu. Novoselov, A.D. Poberezhnikov, E.S. Alyukov. Plasmachemical synthesis and the assessment of the thermal conductivity of fuel compounds “UO2–MgO”, Vol. 2101, 2019, pp. 1–6.